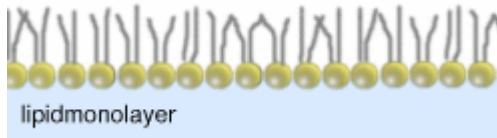


# Another model system: monolayers at the air/water interface

Preparation: spreading of approx. 0.5 mM organic lipid solution on water subphase

Liquid in a Langmuir trough (teflon)

Monolayers are spontaneously formed, reducing the surface tension:



Definition of the surface tension,  $\gamma$

$$\gamma = \left( \frac{\partial G}{\partial A} \right)_{p, T, n}$$

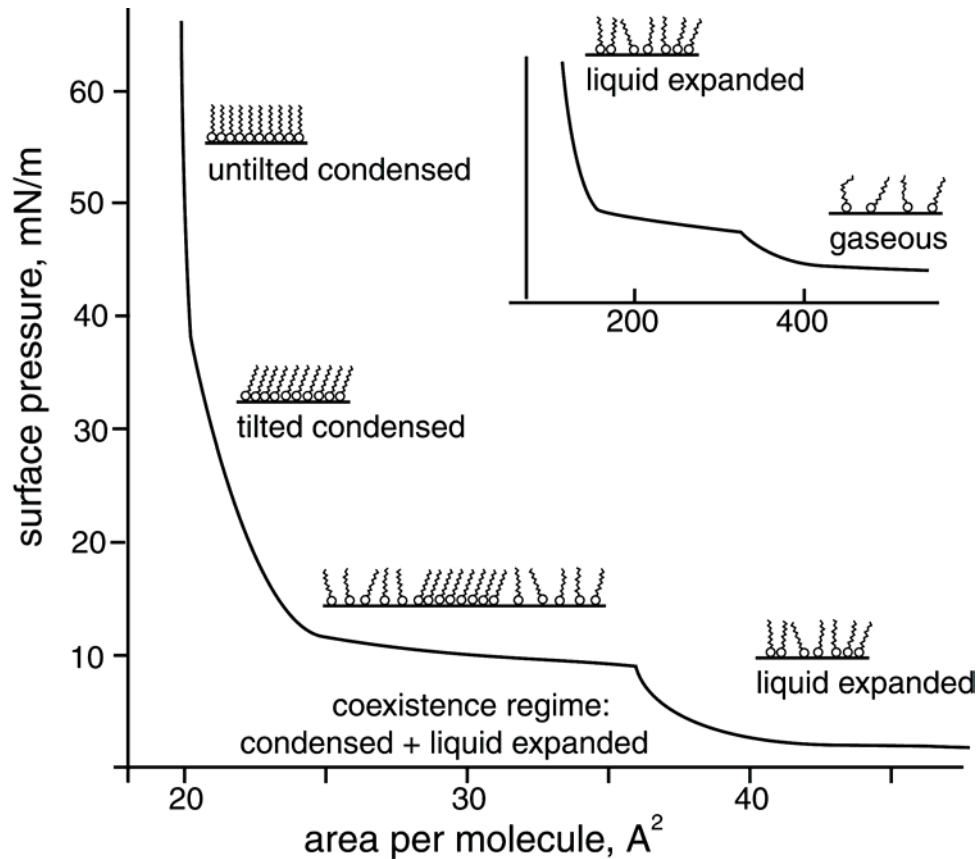
Lateral pressure,  $\pi$

$\gamma_0$ : surface tension clean surface

$\gamma$ : with monolayer

$$\pi = |\gamma - \gamma_0|$$

# phase behavior of monolayers



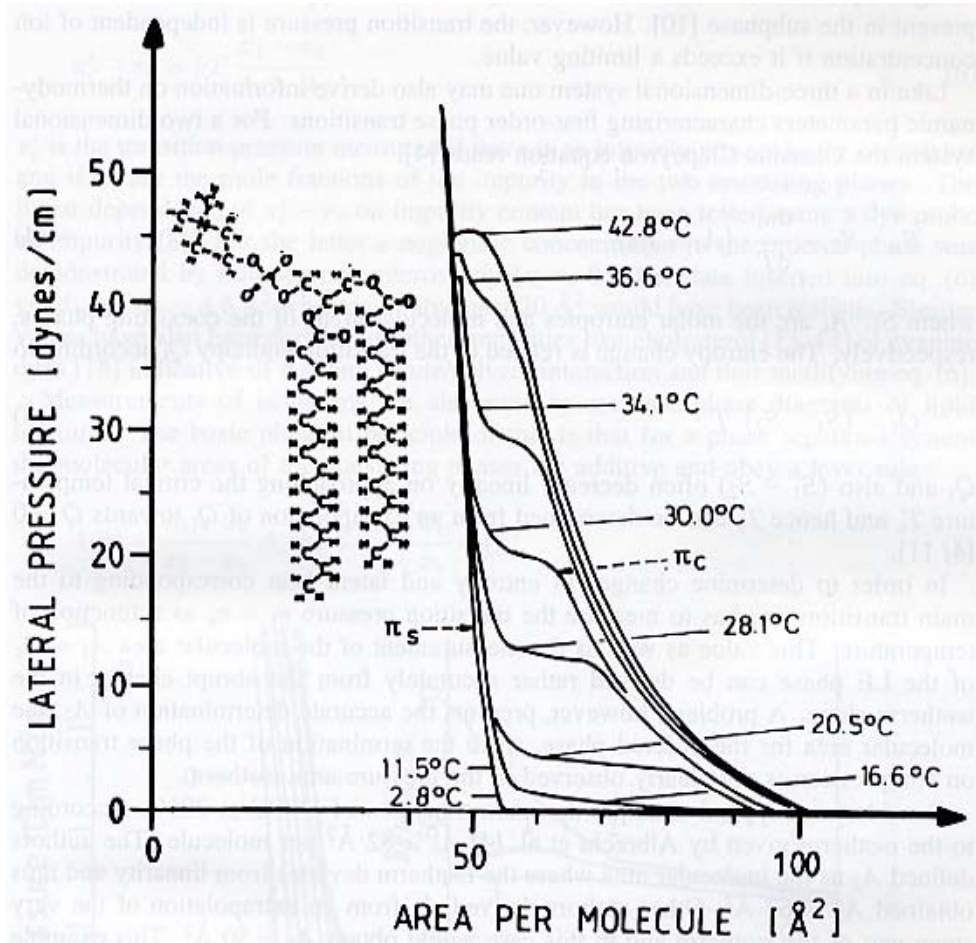
Analogy to 3d phases!  
Gas, liquid, solid

Condensed phases have  
all-trans hydrocarbon  
chains

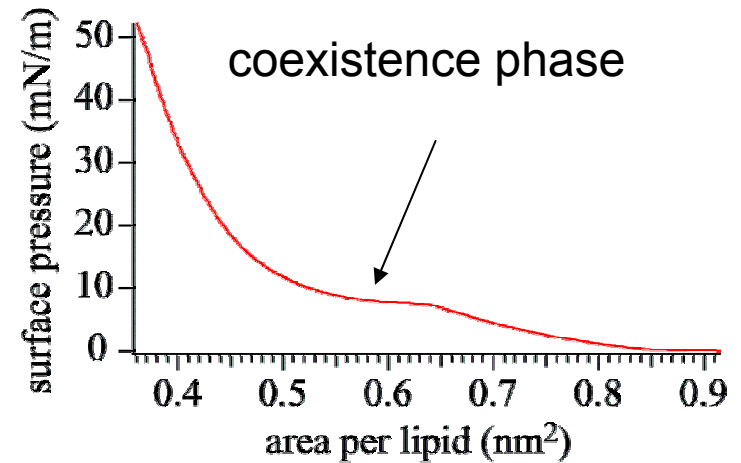
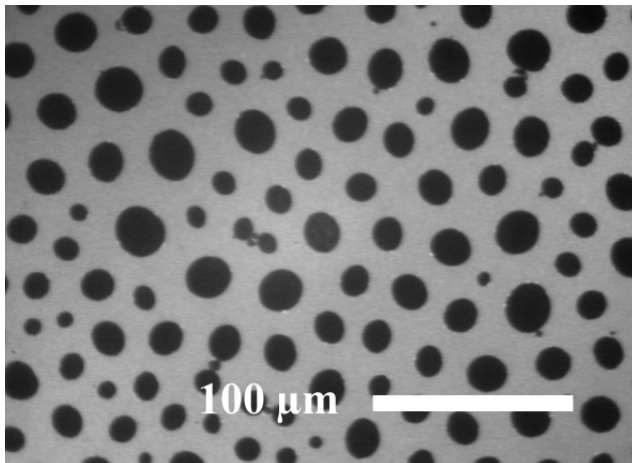
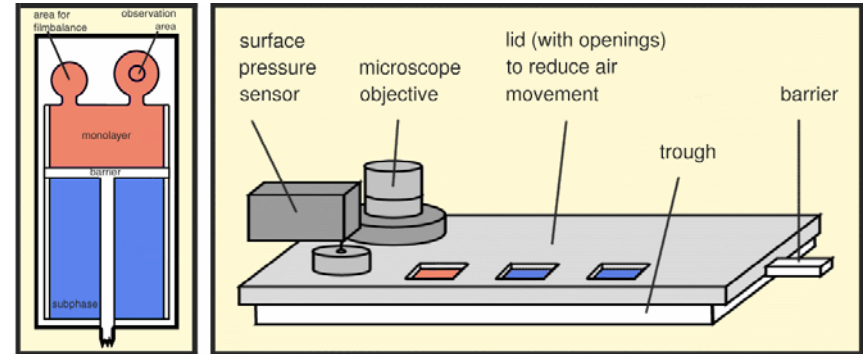
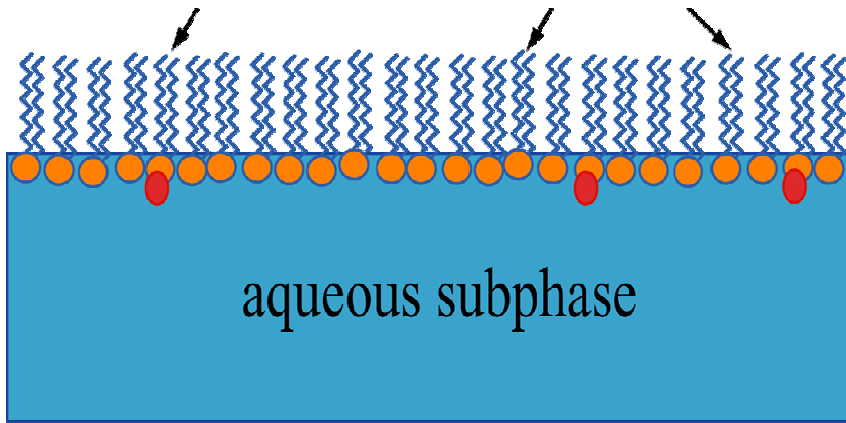
# Dependence on temperature

DPPC on water

Below a temperature threshold, the liquid phase vanishes



# Observation of coexistent phases



# Monolayers on water

Thermodynamic measurements:

-Compressibility  $\chi = -\frac{1}{A} \left( \frac{\partial A}{\partial \pi} \right)$

-isobaric thermal expansivity  $\lambda = \frac{1}{A} \left( \frac{\partial A}{\partial T} \right)_{\pi}$

both functions: derivatives of free energy

-phase transitions are *visible by changes in the slope*: first visible upon compression: liquid-expanded/liquid-condensed (*in DPPC*): first order transition,

*Evidence* extensive purification of the lipid lead to a slope of  $\sim 0$ ,

-adding impurities changes the slope likewise!---

extrapolation: 0.2% impurities present in the DPPC shown

-further compression: at  $A_s$ ,  $\pi_s$ : discontinuous change, 2nd order transition; at lower temperatures: main transition is missing, at  $p_s$  is maintained

– $\pi_s$  is not temperature dependent, can be dependent on counterion content in the subphase, until a threshold value is reached

Clausius-Clapeyron equation for a 2-dimensional system:

$$S_1 - S_2 = \frac{d\pi}{dT}(A_1 - A_2)$$

- S= entropy of phase, A area of phase
- The transition enthalpy is obtained by

$$Q_t = (S_1 - S_2)T$$

- $Q_t$  and  $\Delta S$  decrease often linearly on approaching  $T_c$ , so,  $T_c$  can be obtained by extrapolation of  $Q_t$  towards  $Q=0$ .
- Errors can be made in determining the area As..., not unambiguously to be defined.
- From Raoult's law one can also derive  $A_1-A_2$  : ,  $\pi_c'$ : when there is an impurity present (dye),  $x_i$  are the mole fraction of the impurity in the two phases. Linear dependence on the dye content was tested, relatively small  $\Delta A$  e.g. 6 Angstroms reflects large solvent solute IA

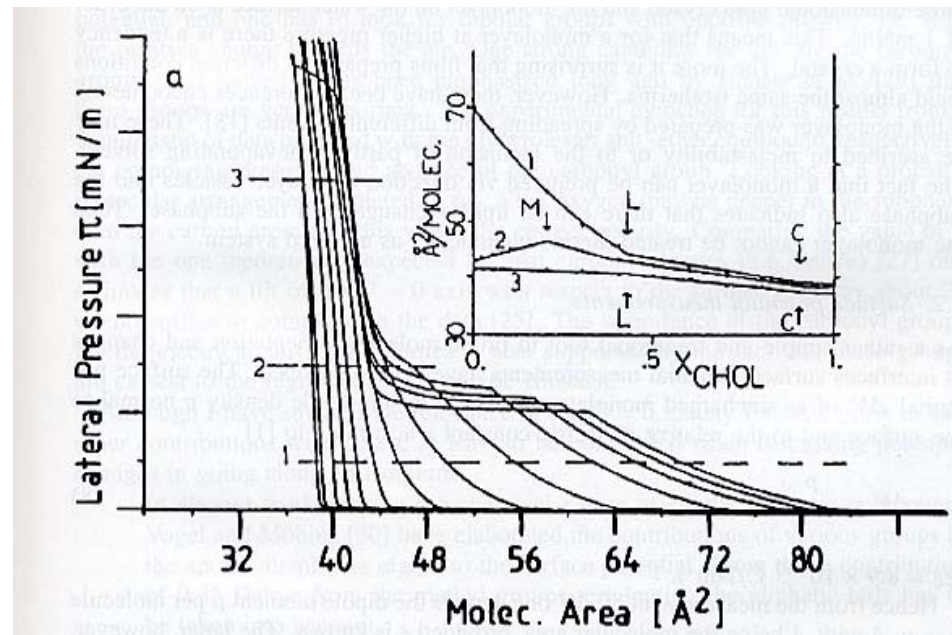
$$\pi_c' - \pi_c = kT \frac{x_1 - x_2}{A_1 - A_2}$$

- Phase diagrams of lipid mixtures: principle: the areas of the both phases are additive and obey a lever rule

$$A(\pi) = \frac{x_1 + x_0}{x_2 - x_1} A_1(\pi) + \frac{x_0 - x_1}{x_2 + x_1} A_2(\pi)$$

- example DMPA/cholesterol phase diagram
- $x_{1,2}$  mole fractions of the one component in the 2 phases,  $x_0$  total content.
- $A(\pi)$  plot vs.  $T$  : extrapolation to  $x_1, x_2$  is possible...composition of the two phases obtained
- At low pressure: two linear slopes
- $X'$  at the change : composition of the mixture with one pure phase...**assumption**  $A(x)$  must be always linear
- Complication: PL monolayer form a metastable equilibrium pressure between a pc crystal and a monolayer at the air-water interface: 1mN/m!!!
- That means: At higher pressures: tendens to form a crystal....interesting: isotherms ARE reproducible!!!
- Other point: different solvents used for spreading can give different isotherms
- Monolayers can also be prepared by injection of vesicles into the subphase! -> no thermodynamically closed system, since lipid exchange with the subphase is possible

## DMPE/Cholesterol mixture isotherms





# Surface potential measurements

Simple and traditional tool (can be sometimes hard to reproduce)

- Surface potential is related to the dipole density  $\rho$  normal to the interface and to the relative dielectric constant  $\varepsilon$

$$\Delta V = \frac{\rho}{\varepsilon\varepsilon_0}$$

- the dipolar moment is obtained from

$$\mu = \rho A$$

- A complication arises since  $\varepsilon$  is not exactly known; (decrease from 80 to 1)

- Consequence: Quantitative interpretation is difficult.

- With charged monolayers: second contribution to  $\Delta V$ 
  - calculation of the possible contribution (Gouy-Chapman-Stern)
  - measurement by respective sensitive dyes (if position is known)

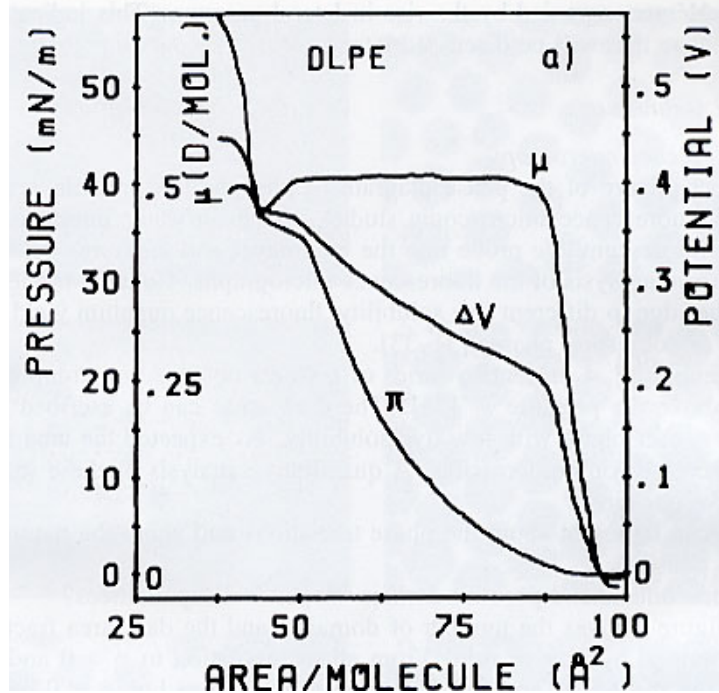
- Properties of uncharged phospholipids:

Expectation: *contribution of highly polar headgroups* dominate the dipolar moment and determine the potential

- Estimation of  $\mu$ :  $\sim 15$  D, but in measurements: only values  $< 1$  D
- Reason: dielectric screening of the groups in water
  
- Dipolar headgroups may also be oriented approx. parallel to the surface, but cationic ammonium groups of PC and PE should be deeper in the subphase than the phosphate residue;
  
- Other possible contributions: -C=O groups
- -CH<sub>3</sub> groups
- free water interface: water at the surface is oriented (can have up to 500 mV)

# Correlation of pressure area isotherms with surface potential (from Miller, Helm, and Möhwald 1987)

## Discussion DLPE



At  $\pi=0$ , meaningless potential, effect of fluctuations

In LE phase:  $\mu$  constant, proportional to  $\mu$

Above  $\pi_c$ : linear slope, less extent, 2 coexisting phases, decrease in  $\mu$ : due to changed orientation in water, reorientation of C=O groups possible

Vogel and Möbius 1988: Dipolar moment in lipids **predominantly caused by terminal CH<sub>3</sub>** groups (0.35 D), minor contribution of headgroups!

Use of CF<sub>3</sub> groups in a carboxylic acid: on decreased tilt (in condensed phase) the surface potential changes likewise (more negative, with CH<sub>3</sub>, it becomes more positive on compression)

Above  $\pi_s$ : possible other phase transition

In the same publication: use of a tip electrode (up to 100 V)  
200  $\mu\text{m}$  above the surface:

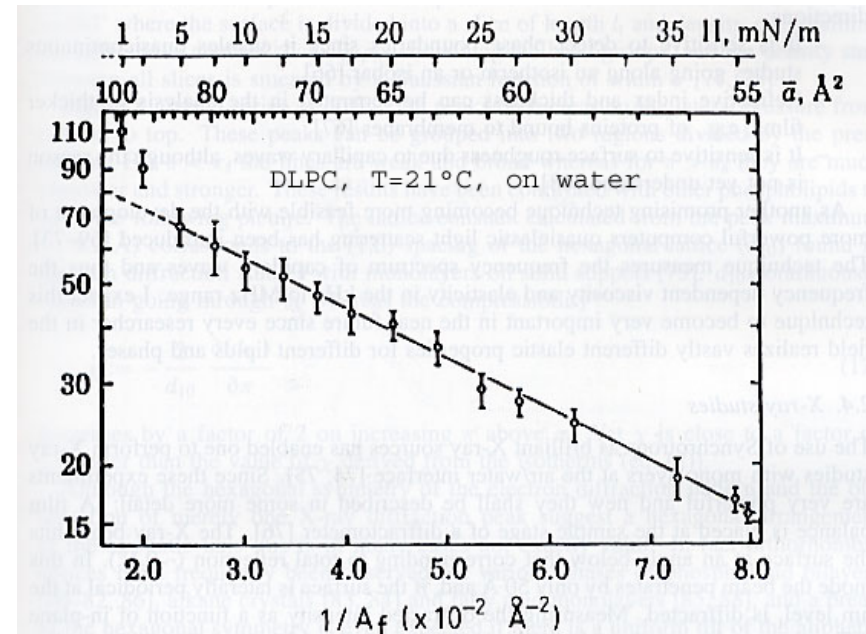
domain repulsion/attraction could be observed by a  
reverse fluorescence microscope;

repulsion/attraction potential was calculated to 6000 kT,  
using  $\mu$  from the potential measurements

Dipolar property of condensed domains proven!

# Fluorescence recovery after photobleaching

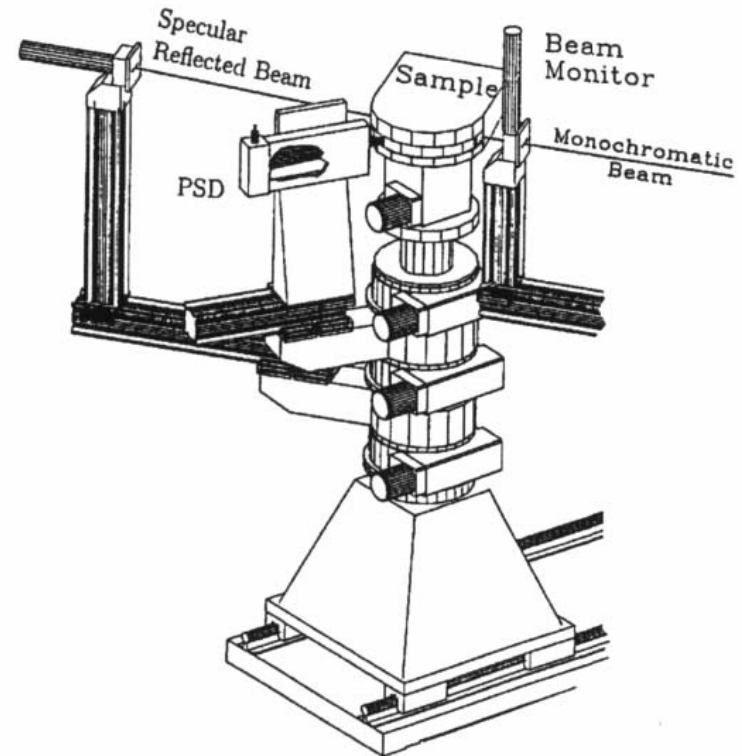
- Principle: photobleaching of a spot, measurement of the fluorescence intensity recovery
- emission recovery of the bleached spot or change in contrast
- Diffusion constants:  
LE phase:  $> 10^{-8}$  cm<sup>2</sup>/s  
LC phase:  $< 10^{-10}$  cm<sup>2</sup>/s
- Applying the free volume model for the motion of small molecules in the membrane (can change place due to free available volume)
- Excellent agreement with the model observed:



$$\ln D = \ln a - \frac{b}{A_f}$$

# Synchrotron X-ray measurements

- Synchrotron radiation enabled to investigate monolayers by x-ray scattering methods: specular reflectivity and grazing incidence x-ray diffraction

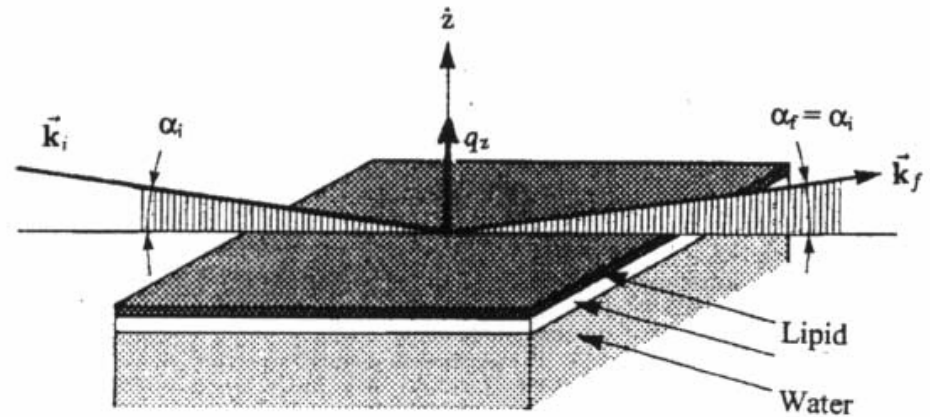


Triple axis spectrometer used for liquid surface scattering at the HASYLAB, DESY, HAMBURG

the electron density across the surface can be calculated using the master formula for reflectivity.

The **master formula** shows only the modulus, not the phases for the function measured.

The reflectivity can be inverted to yield the laterally averaged electron density using a layered model. An electron density model can be built from a stack of slabs. Every slab is assigned to a particular fragment with specific electron density. So, some information about the structure of the lipid becomes available



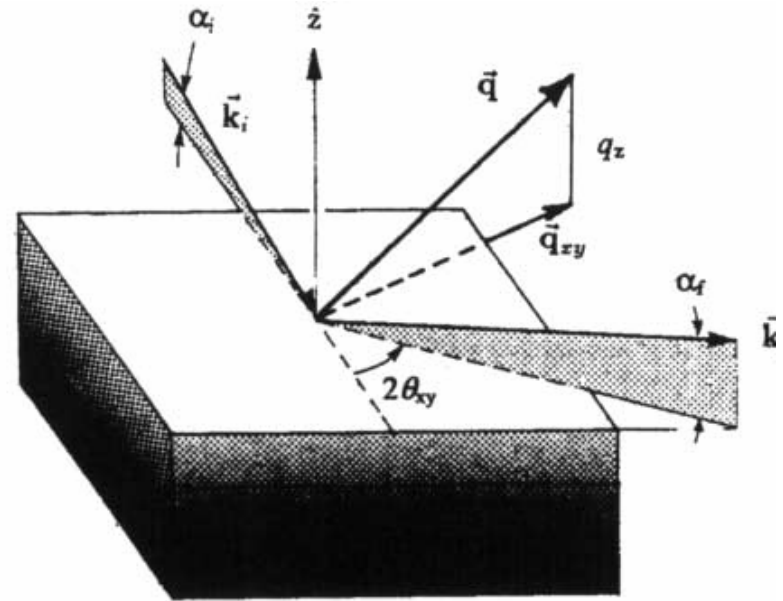
$$\vec{q} \equiv \vec{k}_f - \vec{k}_i, \quad k = 2\pi/\lambda$$

$$\frac{R}{R_F} = \left| \int \frac{d\rho}{dz} \exp(iQ_z) dz \right|^2 \frac{1}{\rho_w}$$

# grazing incidence x-ray diffraction

is performed with  $\lambda = 1.3 \text{ \AA}$ , the critical angle of total reflection  $\alpha_c = 0.13^\circ$ , the incident angle  $\alpha_i = 0.85\alpha_c$ , because of this only a  $90 \text{ \AA}$  thick layer is illuminated by the evanescent wave. The direction of the x-rays are conveniently given by the wave vector  $|\vec{k}_i| = |\vec{k}_f| = k = 2\pi / \lambda$  the scattering process is characterized by the scattering vector  $\vec{q} = \vec{k}_f - \vec{k}_i$  which is separated in a horizontal and vertical component this is, together with the Miller indices used to determine the lattice parameters

$$d = 2\pi / q_{xy}$$

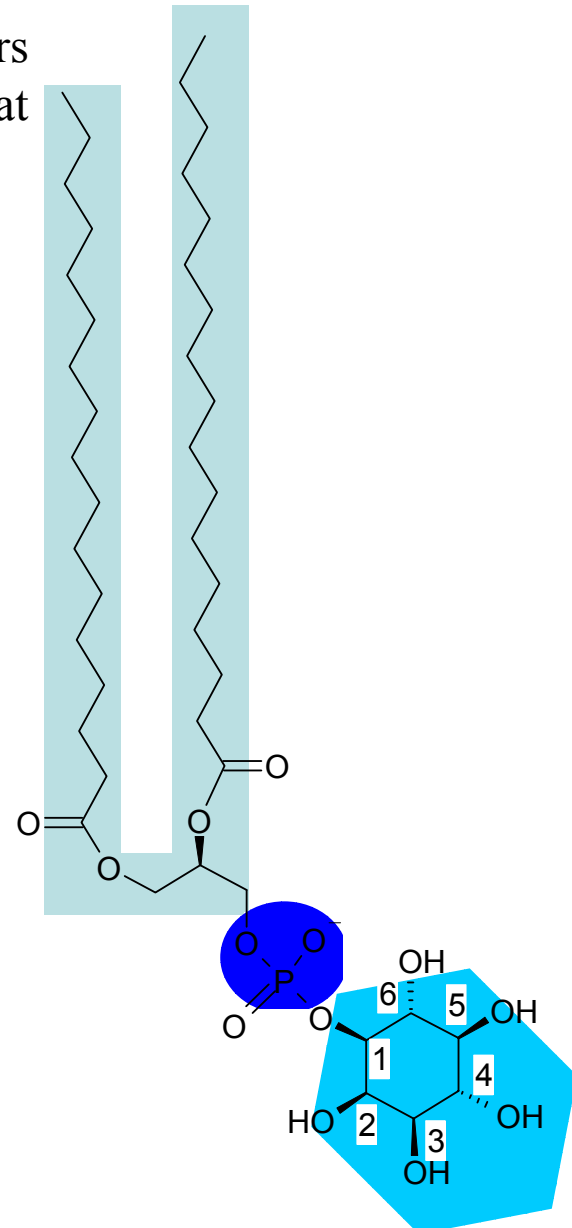
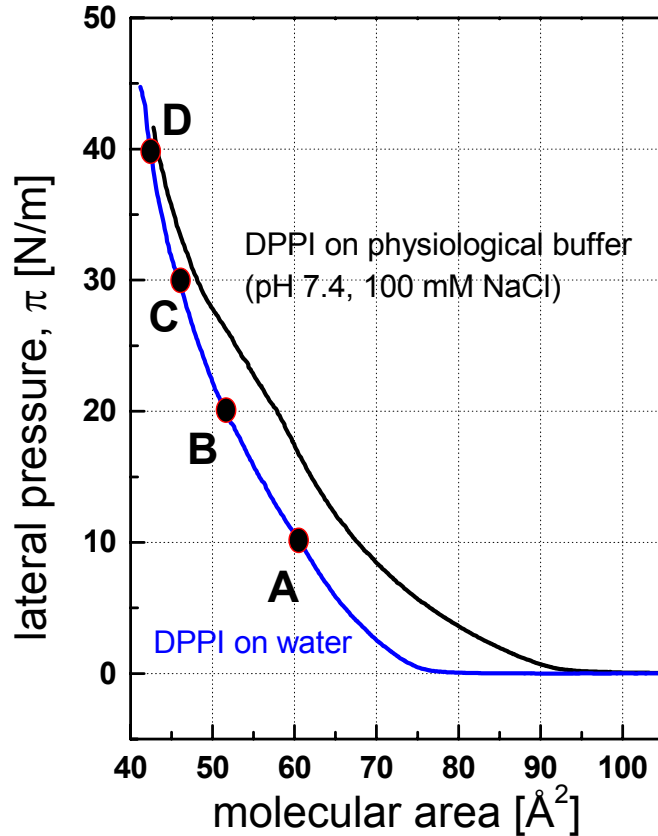


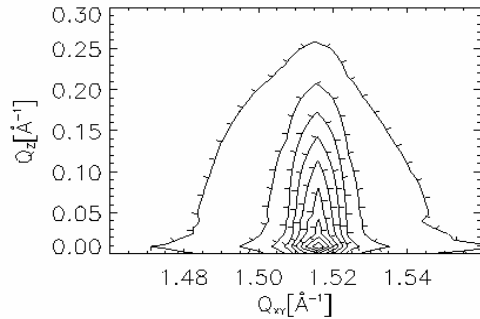
$$\vec{q}_z \approx (2\pi / \lambda) \sin \alpha_f$$

$$q_{xy} \approx 4\pi / \lambda \sin(2\Theta_{xy} / 2)$$



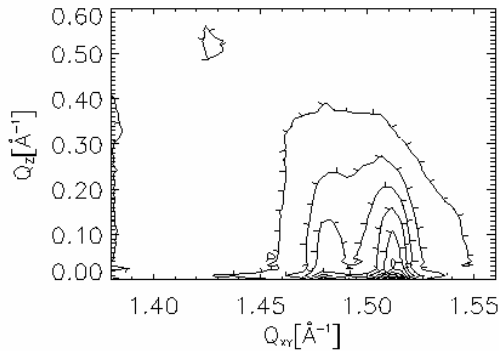
Pressure-area isotherms for DPPI monolayers on pure water and on a physiological buffer at 20 °C.



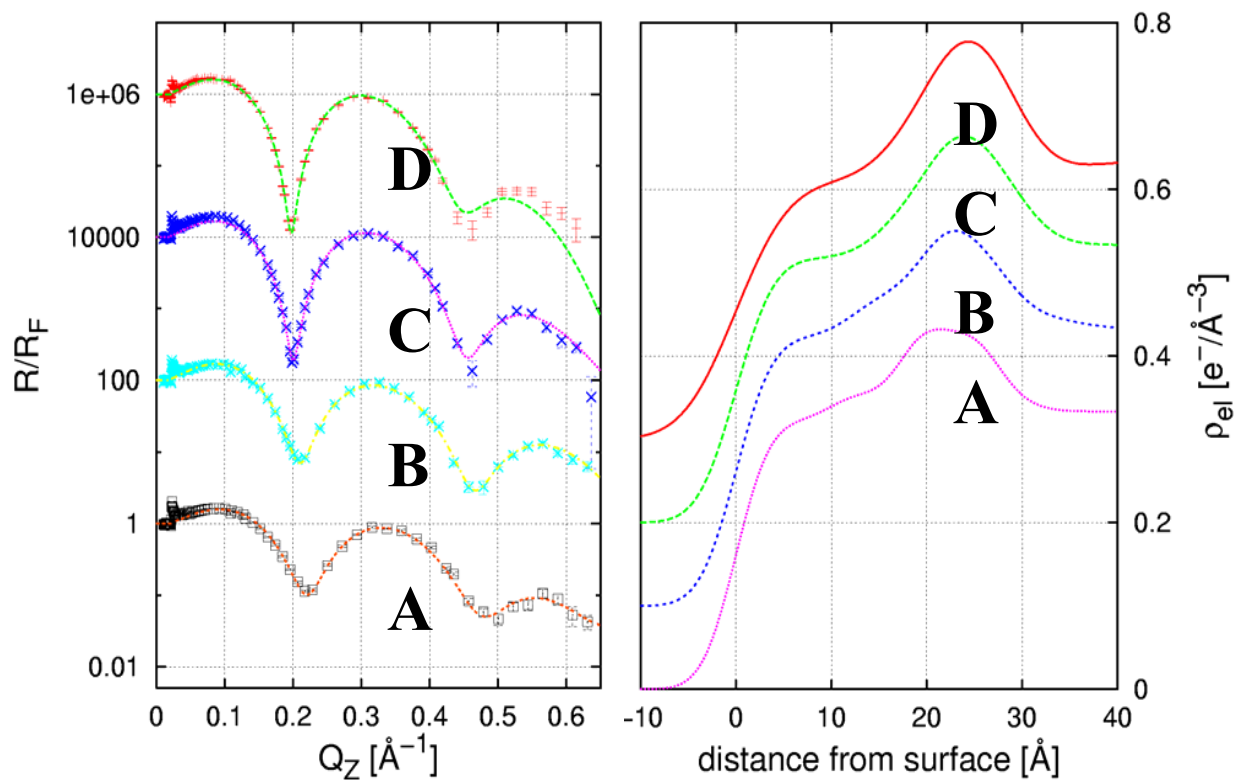


**Examples of GIXD data of DPPI on water (1, upper) and on a physiological buffer (2, lower), both recorded at a lateral pressure of 40 mN/m.**

The diffraction data give direct evidence for minimal molecular area and chain tilt. These parameters obtained by GIXD were complementally used for modelling of the XR data.



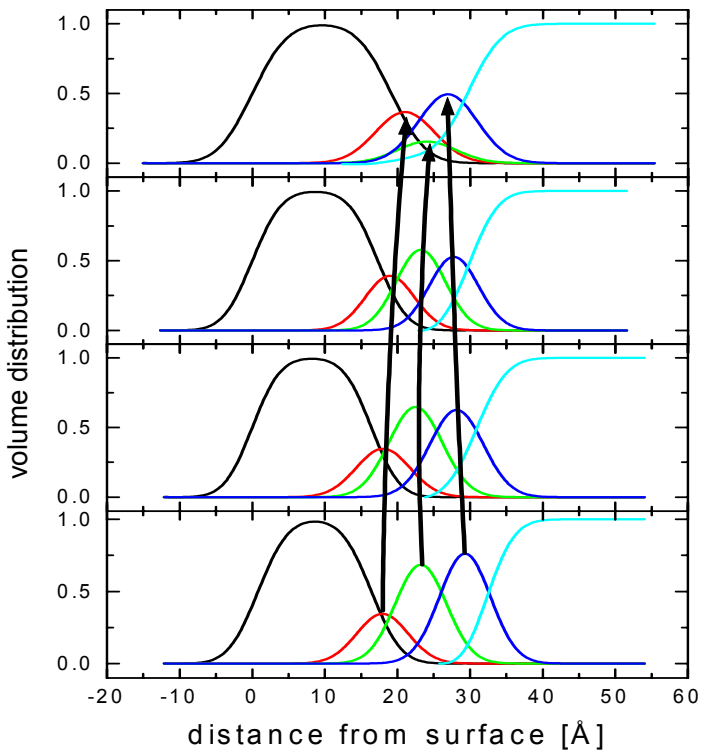
Note that in (2) two phases with different chain tilt are most likely present. At all lateral pressures studied, no homogenous condensed phase was observed for DPPI monolayers on the physiological buffer.



**Left panel:** XR data recorded for monolayers of DPPI on pure water at 20 °C at different lateral pressures (normalized to Fresnel reflectivity of water; A: 10 mN/m, B: 20 mN/m, C: 30 mN/m, D: 40 mN/m). The curves recorded at higher lateral pressures are shifted for better visibility. Best fits obtained are superimposed as lines.

**Right panel:** calculated electron density profiles across the surface normal for the data shown in the left panel. Note the relatively large differences in the head group region in dependence on the lateral pressure in the range of  $\sim 18$ -30  $\text{\AA}$  distance from surface.

Series of volume distributions calculated for each molecular fragment of DPPI.



Here, distributions of the volumes assigned to submolecular fragments across the surface normal calculated for a DPPI monolayer **on water** at 20 °C and varied lateral pressure are depicted. Note that bound water is added to both the phosphate and the inositol fragment. The graphs correspond to the sketches of a structure of DPPI which visualize the results of the calculations. The DPPI molecule apparently undergoes **changes** in both the **headgroup** and the chain organisation when the lateral pressure is varied (on water).